

Communication



Photocatalysis Hot Paper

How to cite: Angew. Chem. Int. Ed. 2025, e202510993 doi.org/10.1002/anie.202510993

Chlorine Radical-Mediated Photocatalytic C—C Coupling of Methanol to Ethylene Glycol with Near-Unity Selectivity

Guang-Xing Dong, Meng-Ran Zhang, Su-Xian Yuan, Min Zhang,* and Tong-Bu Lu*

Abstract: The selective activation of inert C–H bonds in methanol under mild conditions to synthesize high-value C₂ products remains a formidable challenge, primarily due to the competing high reactivity of O-H bonds. Herein, we pioneer a chlorine radical-mediated strategy to redirect the photocatalytic reaction pathway for methanol conversion toward ethylene glycol (EG). Efficient C-H bond activation is achieved by constructing a Z-scheme heterojunction photocatalyst (ZnIn₂S₄/TiO₂-Cl) composed of chlorinated TiO₂ (TiO₂-Cl) and ZnIn₂S₄ with efficient charge separation. Photogenerated holes in this system preferentially oxidize surface-adsorbed Cl- to chlorine radicals (Cl-). These radicals drive a thermodynamically favorable hydrogen atom transfer via hydrogen abstraction, cleaving the C-H bond of methanol to form hydroxymethyl radicals (•CH₂OH). Subsequent C-C coupling of •CH₂OH intermediates, synergistically combined with a self-sustaining Cl⁻/Cl• cycle, produces EG with exceptional selectivity (96.7%) and yield (21.6 mmol g^{-1}) while suppressing overoxidation. In contrast, nonchlorinated catalysts predominantly utilize photogenerated holes for O-H bond cleavage under identical conditions, yielding only C1 products (HCHO, HCOOH). This work not only establishes a solar-driven approach for methanol valorization but also advances mechanistic insights into radical-mediated pathway control in heterogeneous photocatalysis.

Methanol, the simplest monohydric alcohol, is a cornerstone of industrial chemistry, serving as a critical feedstock for energy production, pharmaceuticals, construction materials, and chemical synthesis.^[1,2] Recent advancements have prioritized its upgrading to expand applications, enhance economic viability, and drive sustainable industrial development.^[3–5] Conventional thermal catalytic processes predominantly activate O—H or C—O bonds in methanol, yielding C₁ derivatives

[*] G.-X. Dong, M.-R. Zhang, S.-X. Yuan, Prof. M. Zhang, Prof. T.-B. Lu Institute for New Energy Materials and Low Carbon Technologies, School of Chemistry and Chemical Engineering, Tianjin University of Technology, Tianjin 300384, China E-mail: zm2016@email.tjut.edu.cn

li: zm2016@email.tjut.edu.cn lutongbu@tjut.edu.cn

Additional supporting information can be found online in the Supporting Information section such as formic acid or dimethyl ether. [6-13] However, the selective activation of inert C-H bonds to form C-C linkages—essential for synthesizing high-value multicarbon alcohols like ethylene glycol (EG)—remains a formidable challenge as thermal approaches fail to suppress competing bond cleavage.[14-17] In recent years, numerous studies on photocatalytic methanol conversion have demonstrated that solar-driven photocatalytic technology enables bond activation under mild conditions, making it a sustainable alternative to conventional approaches.[18-29] Notably, certain photocatalysts enable photocatalytic C-H activation to produce EG through precise modulation of composition and structure, steering substrate adsorption selectivity.[26-29] Nevertheless, the intrinsic inertness of C-H bonds and the propensity of photogenerated holes to cleave O-H bonds have hindered progress.

Hydrogen atom transfer (HAT), a thermodynamically driven mechanism involving hydrogen abstraction from C-H bonds by radical acceptors (X•), offers a promising strategy for selective C-H activation. [30] Although reactive oxygen radicals (•OH, •OR) often lead to overoxidation, [31] halogen radicals such as Cl. exhibit superior selectivity due to their higher bond dissociation energies (BDEs) compared to C-H bonds (see Table S1).[32-36] Despite this potential, Cl--mediated photocatalytic systems for methanol-to-EG conversion remain unexplored. To demonstrate this concept, we engineered a Z-scheme heterojunction photocatalyst. ZnIn₂S₄/TiO₂-Cl, to redirect photocatalytic methanol dehydrogenation pathways. The formation of a Z-scheme heterojunction promotes the separation of photogenerated charge carriers while retaining strong redox potential. Critically, chlorinated TiO₂-Cl generates Cl• radicals under irradiation, which selectively abstract hydrogen from the C-H bond of methanol, forming •CH₂OH intermediates. Subsequent radical coupling produces EG with 96.7% selectivity and a yield of 21.6 mmol g⁻¹, with concurrent chlorine regeneration ensuring catalytic stability. Conversely, nonchlorinated analogs favor C₁ products (e.g., HCHO and HCOOH).

Individual ZnIn $_2$ S $_4$ and TiO $_2$ (before and after chlorination) were synthesized according to previously reported methods. The composites, ZnIn $_2$ S $_4$ /TiO $_2$ and ZnIn $_2$ S $_4$ /TiO $_2$ -Cl, were prepared via an in situ loading strategy (see Scheme S1 for synthesis details). Transmission electron microscopy (TEM) analysis revealed that both TiO $_2$ and TiO $_2$ -Cl exhibit an irregular sheet-like morphology with an average lateral size of 15–20 nm, confirming that chlorination minimally affects TiO $_2$ morphology (Figure 1a–c). Pristine ZnIn $_2$ S $_4$ displays nanosheet morphology (Figure 1d), whereas

15213773, 0, Downloaded from https://onlinelibrary.wiley.com/doi/10.1002/anie.202310993 by Tianjin University Of, Wiley Online Library on [24.062025]. See the Terms and Conditions (https://onlinelibrary.wiley.com/terms-and-conditions) on Wiley Online Library for rules of use; OA articles are governed by the applicable Creative Commons. Licenson

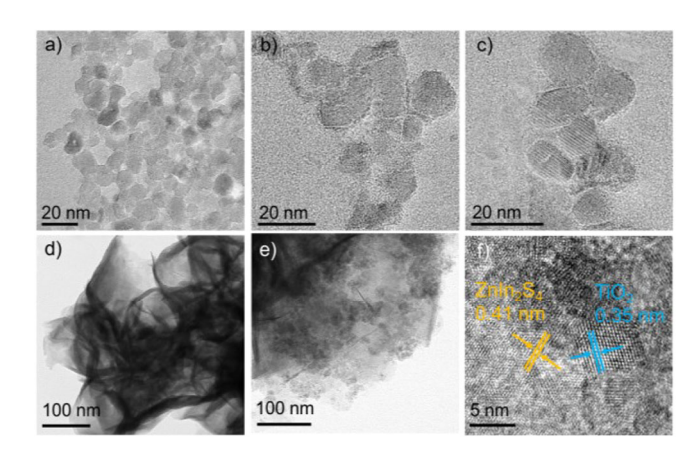


Figure 1. TEM images of a) and b) TiO2, c) TiO2-Cl, d) ZnIn2S4, and e) ZnIn₂S₄/TiO₂-Cl. f) HRTEM image of ZnIn₂S₄/TiO₂-Cl.

ZnIn₂S₄/TiO₂-Cl demonstrates well-dispersed TiO₂-Cl sheets anchored on ZnIn₂S₄ nanosheets (Figure 1e). High-resolution TEM (HRTEM) imaging further identified distinct lattice fringes with spacings of 3.5 and 4.1 Å, matching the (101) plane of anatase TiO₂ and the (006) plane of hexagonal ZnIn₂S₄, respectively (Figure 1f), thereby verifying the successful formation of the heterojunction. Energy-dispersive X-ray spectroscopy (EDS) elemental mapping demonstrated homogeneous distribution of Zn, In, S, Ti, O, and Cl across the related surfaces of TiO2, TiO2-Cl, ZnIn2S4, and ZnIn₂S₄/TiO₂-Cl (Figures S1–S4), supporting the effective synthesis of both pristine and composite materials. X-ray diffraction (XRD) patterns (Figure S5) confirmed that pristine ZnIn₂S₄ and TiO₂ are in good agreement with their standard reference data (JCPDS No. 65-2023 for ZnIn₂S₄ and No. 21-1272 for TiO₂).^[37,39] Notably, the XRD profile of TiO₂-Cl remained nearly identical to pristine TiO₂, indicating that chlorination preserves the anatase crystalline structure. [38] For the ZnIn₂S₄/TiO₂-Cl composite, the coexistence of characteristic diffraction peaks from both components further validates the successful integration of TiO2-Cl with ZnIn₂S₄.

Photocatalytic methanol conversion reactions were conducted in a custom-built distillation reactor (Figures 2a and S6), which collects high-boiling-point products at the bottom to minimize overoxidation. As shown in Figure 2b, pristine TiO₂ primarily produced C₁ derivatives (HCHO and HCOOH) with trace CO2, indicating poor selectivity toward C-C coupling. The ZnIn₂S₄/TiO₂ composite exhibited analogous catalytic behavior, with enhanced C₁ product yields (e.g., HCHO increased from 0.2 to 1.6 mmol g^{-1}). However, no detectable C2 products such as EG were observed, suggesting that photogenerated holes alone are insufficient to drive methanol coupling. In contrast, using chlorinated TiO₂ (TiO₂-Cl) as the catalyst achieved significant EG production (2.9 mmol g⁻¹, 94.5% selectivity) with negligible CO₂ generation, highlighting its superior C—C coupling capability. Meanwhile, it was observed that the chlorine content in TiO₂-Cl exhibited a time-dependent relationship with the chlorination time, reaching equilibrium at 24 h (Figure S7a). Additionally, the photocatalytic activity for EG production

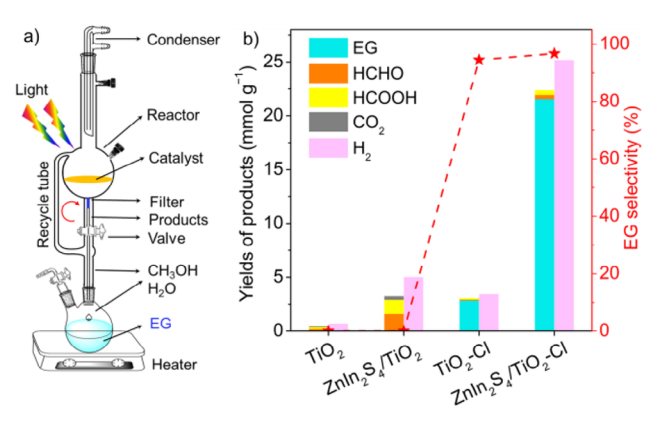


Figure 2. a) Schematic of the reaction system. b) Product yields using different photocatalysts, with EG selectivity calculated as: selectivity = n(EG)/(n(EG) + n(HCHO) + n(HCOOH)), where n(EG), n(HCHO), and n(HCOOH) represent the yields of EG, HCHO and HCOOH, respectively.

was positively correlated with the chlorine content (Figure S7b). Therefore, a 24-h chlorination treatment was optimal for achieving maximum equilibrium chlorine content on the catalyst surface, thereby enhancing photocatalytic activity. By integrating TiO2-Cl with ZnIn2S4 to form a Z-scheme heterojunction, the EG yield surged to 21.6 mmol g⁻¹ (96.7% selectivity), outperforming standalone TiO₂-Cl by nearly an order of magnitude. Notably, H2 was consistently detected as the sole reduction product via gas chromatography across all catalytic systems. Further, calculations on the electronhole consumption ratio (e⁻/h⁺) revealed that the values of e⁻/h⁺ for all photocatalytic systems are close to 1 (Table S2), confirming the stability of the reduction pathway. Moreover, the chlorinated samples exhibited a significantly reduced yield and selectivity for the high-boiling-point product EG, alongside increased H₂ production, compared to the distillation system (Figure S8a,b). This trend indicates that EG undergoes further oxidation, highlighting the unique advantage of the custom-built distillation reactor in suppressing overoxidation of high-boiling-point products.

To elucidate the marked differences in product selectivity between chlorinated and nonchlorinated catalysts, intermediate trapping measurements were performed to probe the underlying reaction pathways. Electron paramagnetic resonance (EPR) spin-trapping experiments with 5,5-dimethyl-1pyrroline-N-oxide (DMPO) as trapping agent confirmed that catalysts are indispensable for initiating radical generation. In nonchlorinated systems (TiO₂ and ZnIn₂S₄/TiO₂), only the DMPO-OCH₃ adduct signal was detected (Figure 3a), indicating dominant O-H bond cleavage generating methoxy radicals (CH₃O•), critical intermediates for C₁ product formation (HCHO and HCOOH). In contrast, chlorinated systems (TiO₂-Cl and ZnIn₂S₄/TiO₂-Cl) predominantly exhibited the DMPO-CH₂OH adduct signal (Figure 3b), demonstrating preferential C-H bond activation to form hydroxymethyl radicals (•CH₂OH), essential for EG synthesis. Notably, both composite catalysts (ZnIn₂S₄/TiO₂ and ZnIn₂S₄/TiO₂-Cl) show stronger EPR signals than their standalone counterparts, aligning with their enhanced photocatalytic activities.

15213773, 0, Downloaded from https://onlinelibrary.wiley.com/doi/10.1002/anie.202310993 by Tianjin University Of, Wiley Online Library on [24.062025]. See the Terms and Conditions (https://onlinelibrary.wiley.com/terms-and-conditions) on Wiley Online Library for rules of use; OA articles are governed by the applicable Creative Commons. Licenson

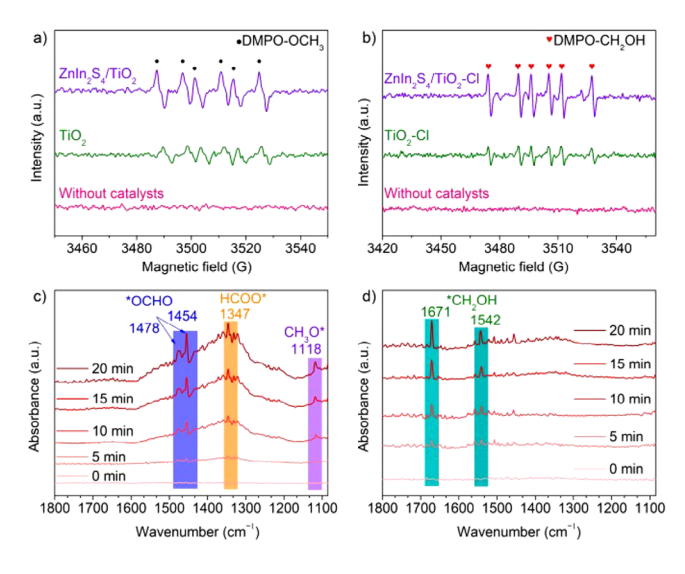


Figure 3. EPR spectra of a) DMPO-OCH₃ and b) DMPO-CH₂OH. In situ FTIR spectra under different light irradiation times on c) ZnIn₂S₄/TiO₂ and d) ZnIn₂S₄/TiO₂-Cl.

Complementing the EPR findings, in situ Fourier transform infrared (FTIR) spectroscopy further elucidated the reaction pathways. For ZnIn₂S₄/TiO₂, time-dependent spectra (Figure 3c) revealed intensified peaks at 1118 cm⁻¹ (CH₃O•), 1347 cm⁻¹ (HCOO•), 1478 cm⁻¹ and 1454 cm⁻¹ (•OCOH), aligning with the C₁ product pathway. [40] Conversely, the FTIR spectrum of ZnIn₂S₄/TiO₂-Cl displays prominent peaks at 1542 cm⁻¹ and 1671 cm⁻¹, assigned to •CH₂OH intermediates (Figure 3d).[41] These results unequivocally establish that chlorine incorporation redirects the reaction pathway from O-H to C-H bond activation, enabling selective EG synthesis via •CH2OH coupling.

X-ray photoelectron spectroscopy (XPS) measurements were further performed to investigate surface elemental evolution. The O 1s spectrum (Figure S9a) exhibits two distinct peaks: a high-binding-energy peak attributed to lattice oxygen (Olatt) and a low-binding-energy peak corresponding to surface-adsorbed H₂O/hydroxyl groups (O_{ads}).^[42] Chlorination time-dependently suppressed the O_{ads} signal, indicating progressive surface oxygen depletion. Concurrently, the Cl 2p spectrum (Figure S9b) revealed two peaks at 198.0 eV (Cl $2p_{3/2}$) and 199.5 (Cl $2p_{1/2}$). The peak observed at 198.0 eV can be attributed the formation of Ti-Cl bonds, [43] supporting a substitution mechanism involving Cl- replacing surface oxygen species (HCl + HO - Ti \rightarrow Ti-Cl + H₂O). [44,45] To validate the generation of Cl. radicals, molecular trapping experiment utilizing N,N-diallyl-4-methylbenzenesulfonamide as a probe molecule was conducted under light irradiation. In the ZnIn₂S₄/TiO₂-Cl system, ¹H and ¹³C NMR analyses revealed the characteristic signals of the radical cyclizationderived adduct (Figure S12). This observation provides unambiguous evidence for the formation of Cl. radicals during the photocatalytic process.[46,47] Complementarily, EPR studies using *N-tert*-butyl-alpha-phenylnitrone (PBN) detected a PBN-CHOH-Cl signal in the ZnIn₂S₄/TiO₂-Cl system (Figure S13), directly evidencing the transient Cl• and •CH2OH radicals. These data collectively demonstrate

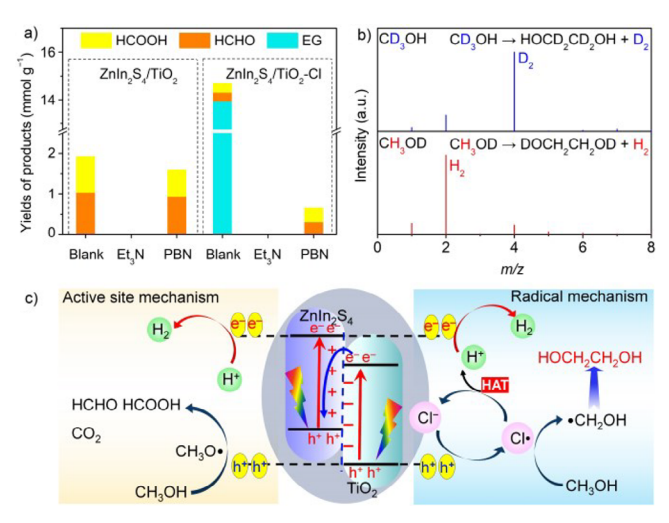


Figure 4. a) Yields of products with ZnIn₂S₄/TiO₂ or ZnIn₂S₄/TiO₂-Cl as the photocatalyst under different quenchers. b) Mass spectra of H₂ generated over ZnIn₂S₄/TiO₂-Cl with CD₃OH or CH₃OD as feedstocks. c) Schematic diagram of the proposed reaction pathway for CH₃OH conversion with ZnIn₂S₄/TiO₂ or ZnIn₂S₄/TiO₂-Cl as the photocatalyst.

that photogenerated holes oxidize surface Cl⁻ to Cl• radicals, which subsequently abstract hydrogen from C-H bonds of methanol to form •CH₂OH intermediates. Crucially, postreaction XPS analysis and chlorine content detected confirmed stable Cl retention on the catalyst surface (Figures S14 and \$15), validating efficient chlorine cycling within the system. Moreover, repeated experiments showed that ZnIn₂S₄/TiO₂-Cl retained a consistent EG yield over three cycles (Figure S16), demonstrating the stability of chlorine cycling and the photocatalytic process.

To validate the proposed mechanism, systematic radical scavenging experiments were conducted. As shown in Figure 4a, adding triethylamine (Et₃N), a hole scavenger, completely suppressed methanol conversion in both ZnIn₂S₄/TiO₂ and ZnIn₂S₄/TiO₂-Cl systems, confirming the essential role of photogenerated holes. When PBN was introduced to scavenge CI. radicals, the nonchlorinated ZnIn₂S₄/TiO₂ system retained its C₁ product distribution. In contrast, the chlorinated ZnIn₂S₄/TiO₂-Cl catalyst exhibited near-complete suppression of EG production (<5% yield) with residual C₁ species (HCHO/HCOOH). This stark contrast implies that Cl. radicals (selectively generated in chlorinated systems) are indispensable for C-H activation and subsequent C-C coupling toward EG, whereas their absence redirects oxidation pathways to O-H cleavage for C₁ products. To trace the hydrogen origin in EG synthesis, isotope labeling experiments were conducted using CD₃OH and CH₃OD. Mass spectrometry analysis (Figure 4b) revealed exclusive D_2 evolution (m/z = 4) from CD_3OH and predominant H_2 generation (m/z = 2) from CH_3OD , definitively establishing that H₂/D₂ originates from C-H bond cleavage rather than O-H bonds. This confirms EG formation via C-H activation followed by C-C coupling. Kinetic isotope effect (KIE) studies further corroborated C-H bond cleavage as the rate-determining step (RDS), with KIE values (k_H/k_D) of 7.52 (TiO₂-Cl) and 8.55 (ZnIn₂S₄/TiO₂-Cl) (Figure S17).[48,49]

15213773, 0, Downloaded from https://onlinelibrary.wiley.com/doi/10.1002/anie.202310993 by Tianjin University Of, Wiley Online Library on [24.062025]. See the Terms and Conditions (https://onlinelibrary.wiley.com/terms-and-conditions) on Wiley Online Library for rules of use; OA articles are governed by the applicable Creative Commons. Licenson



These large KIE values (>5) align with C–H bond activation as the RDS, solidifying the critical role of chlorination in steering methanol dehydrogenation toward C-H bond rupture.

To elucidate the enhanced photocatalytic performance of the ZnIn₂S₄/TiO₂-Cl heterojunction, we systematically analyzed its band structure and charge transfer dynamics. UV-vis diffuse reflectance spectroscopy (DRS) data (Figure \$18a) revealed a slight redshift in the absorption edge of TiO₂-Cl compared to pristine TiO₂, attributed to chlorination-induced oxygen vacancies, as confirmed by EPR spectra (Figure S19). Although pristine ZnIn₂S₄ exhibited broad visible-light absorption up to 516 nm, the ZnIn₂S₄/TiO₂-Cl composite combined the absorption edges of both components, achieving enhanced light utilization across a broader spectrum. Tauc plot analysis (Figure S18b) determined bandgap energies of 2.81 eV for TiO₂-Cl and 2.21 eV for ZnIn₂S₄. Mott-Schottky measurements (Figure \$18c.d) further revealed conduction band minimum potentials ($E_{\rm CB}$) of $-0.60~{\rm V}$ and $-1.05~{\rm V}$ versus the standard hydrogen electrode (SHE) for TiO2-Cl and ZnIn₂S₄, respectively. Consequently, the valence band maximum potentials (E_{VB}) were calculated as 2.21 V (TiO₂-Cl) and 1.16 V (ZnIn₂S₄) versus SHE, respectively. The resultant staggered band alignment (Figure S20) facilitates efficient charge separation, consistent with the observed photocatalytic enhancement.

High-resolution XPS analysis of the ZnIn₂S₄/TiO₂-Cl heterojunction (Figure S21) revealed distinct binding energy shifts compared with the individual components: a positive shift of 0.3 eV for In 3d and a negative shift of 0.25 eV for Ti 2p. These shifts indicate net electron transfer from ZnIn₂S₄ to TiO₂-Cl upon interfacial contact, generating an interfacial built-in electric field that facilitates photogenerated carrier separation. In situ illuminated XPS (Figure S22) further confirmed the Z-scheme photogenerated charge transfer mechanism: under light irradiation, the In 3d binding energy shifted negatively (electron accumulation in ZnIn₂S₄), whereas the Ti 2p binding energy shifted positively (hole retention in TiO₂-Cl). These observations directly support that photogenerated electrons from TiO₂-Cl recombine with photogenerated holes from ZnIn₂S₄, preserving the high redox potentials of both components—ZnIn₂S₄ electrons (-1.05 V versus SHE) for H₂ evolution and TiO₂-Cl holes (2.21 V versus SHE) for Cl⁻ oxidation. Transient photocurrent responses and electrochemical impedance spectroscopy (EIS) measurements (Figure S23a,b and Table S3) validated enhanced charge kinetics, with the heterojunction exhibiting a 1.84-fold increase in photocurrent density and a 46.7% reduction in charge transfer resistance compared to standalone components. These synergistic effects collectively enhance Cl• radical production, driving efficient C-H activation and selective photocatalytic conversion.

Based on the mechanistic insights and structure-activity relationships elucidated above, distinct reaction pathways are proposed for methanol conversion over chlorinated and nonchlorinated catalysts, as schematically illustrated in Figure 4c. In both systems, photogenerated carriers in the ZnIn₂S₄/TiO₂ and ZnIn₂S₄/TiO₂-Cl heterojunctions follow a Z-scheme transfer mechanism. However, chlorination induces a fundamental divergence in surface chemistry, manifested through two distinct mechanisms: 1) nonchlorinated system (active site mechanism): unrecombined photogenerated holes migrate to the catalyst surface, acting as the primary oxidizing species. Due to the lower activation energy of O-H bond cleavage compared to C-H bond activation in methanol, these holes preferentially oxidize O-H bonds, generating CH₃O• radicals. Sequential oxidation of CH₃O• yields C₁ products (HCHO and HCOOH), whereas photogenerated electrons reduce protons to H₂. Trace CO₂ is produced via partial overoxidation of intermediates. 2) Chlorinated system (radical-mediated mechanism): surfaceadsorbed Cl⁻ alters the oxidation hierarchy. The ionization energy (IE) of Cl^- ($Cl^- \rightarrow Cl^{\bullet} + e^-$; IE = 3.61 eV) is significantly lower than the first IE of methanol (CH₃OH → CH_3OH^+/CH_3OH^\bullet IE = 10.84 eV), [50,51] indicating that $Cl^$ is thermodynamically favored for oxidation. Consequently, photogenerated holes in TiO₂-Cl preferentially oxidize Cl⁻ to Cl. radicals. These Cl. radicals selectively abstract hydrogen from the C-H bond of methanol via HAT, forming •CH₂OH radicals. Subsequent C–C coupling of •CH₂OH intermediates produces EG with 96.7% selectivity. The resultant Cl⁻ is efficiently readsorbed on the TiO2 surface, enabling a closed chlorine cycling (Cl-/Cl•).[52] This cycle suppresses holemediated overoxidation, thereby inhibiting CO₂ formation. This interfacial decoupling of hole activity from direct substrate oxidation redirects the reaction pathway toward selective C-H activation and C-C coupling. This strategy highlights the unique advantage of chlorine radical-mediated catalysis in steering reaction selectivity toward high-value multicarbon products.

In summary, we have demonstrated a chlorine-engineered Z-scheme ZnIn₂S₄/TiO₂-Cl heterojunction that achieves selective photocatalytic methanol-to-EG conversion under ambient conditions. Surface chlorination redirects methanol dehydrogenation pathways from thermodynamically favored C₁ products (HCHO/HCOOH) to C₂ EG, delivering an exceptional yield of 21.6 mmol g⁻¹ with 96.7% selectivity. EPR, in situ FTIR, isotope labeling, and scavenging experiments collectively revealed a radical-mediated dichotomy in the reaction pathways. Nonchlorinated systems prioritize O-H cleavage by photogenerated holes, yielding C1 derivatives. Chlorinated systems leverage Cl. radicals (via hole-induced Cl⁻ oxidation) for selective C-H activation via HAT, enabling •CH2OH coupling to EG while suppressing CO₂ formation. The Z-scheme charge transfer enhances carrier separation, as evidenced by photophysical characterization, whereas the Cl-/Cl• cycle acts as a hole scavenger to prevent overoxidation. This strategy establishes a solar-driven, atom-efficient route for EG synthesis, circumventing energy-intensive thermal processes and offering a paradigm for selective C-C coupling in photocatalytic biomass valorization.

Acknowledgements

This work was financially supported by the National Key R&D Program of China (2022YFA1502902), the NSFC

15213773, Q. Downloaded from https://onlinelibrary.wiley.com/doi/10.1002/anie.202510993 by Tianjin University Of, Wiley Online Library on [24.062025]. See the Terms and Conditions (https://onlinelibrary.wiley.com/terms-and-conditions) on Wiley Online Library or rules of use; OA articles are governed by the applicable Creative Commons.



(22475152 and U21A20286), the Natural Science Foundation of Tianjin City (24JCYBJC00840), and the 111 Project of China (D17003).

Conflict of Interests

The authors declare no conflict of interest.

Data Availability Statement

The data that support the findings of this study are available from the corresponding author upon reasonable request.

Keywords: C-H activation • CH₃OH conversion • Charge separation • Photocatalysis • Radical-mediated reaction pathway

- [1] H. Wang, E. Harkou, A. Constantinou, S. M. Al-Salemc, G. Manos, J. Tang, Chem. Soc. Rev. 2025, 54, 2188-2207.
- X. Wu, Y. Wei, Z. Liu, Acc. Chem. Res. 2023, 56, 2001–2014.
- [3] H. Wang, H. Qi, X. Sun, S. Jia, X. Li, T. J. Miao, L. Xiong, S. Wang, X. Zhang, X. Liu, A. Wang, T. Zhang, W. Huang, J. Tang, Nat. Mater. 2023, 22, 619-626.
- [4] C. Filosa, X. Gong, A. Bavykina, A. D. Chowdhury, J. M. R. Gallo, J. Gascon, Acc. Chem. Res. 2023, 56, 3492-3503.
- [5] T. T. Le, W. Qin, A. Agarwal, N. Nikolopoulos, D. Fu, M. D. Patton, C. Weiland, S. R. Bare, J. C. Palmer, B. M. Weckhuysen, J. D. Rimer, Nat. Catal. 2023, 6, 254–265.
- [6] W. Chen, J. Zuo, K. Sang, G. Qian, J. Zhang, D. Chen, X. Zhou, W. Yuan, X. Duan, Angew. Chem. Int. Ed. 2024, 63, e202314288.
- [7] F. Liu, X. Yi, T. Liu, W. Chen, J. Yang, Y. Xiao, Y. Qin, L. Song, A. Zheng, Sci. Adv. 2025, 11, eads4018.
- [8] X. Wang, X. Gao, F. Song, X. Wang, G. Cao, J. Zhang, Y. Han, O. Zhang, ACS Catal. 2024, 14, 1093-1097.
- [9] Q. Fang, S. Ye, L. Zheng, H. Wang, L. Hu, W. Gu, L. Wang, L. Shi, C. Zhu, ACS Catal. 2024, 14, 9235–9243.
- [10] A. Cesarini, S. Mitchell, G. Zichittella, M. Agrachev, S. P. Schmid, G. Jeschke, Z. Pan, A. Bodi, P. Hemberger, J. Pérez-Ramírez, Nat. Catal. 2022, 5, 605-614.
- [11] Y. Zhou, S. Santos, M. Shamzhy, M. Marinova, A.-M. Blanchenet, Y. G. Kolyagin, P. Simon, M. Trentesaux, S. Sharna, O. Ersen, V. L. Zholobenko, M. Saeys, A. Y. Khodakov, V. V. Ordomsky, Nat. Commun. 2024, 15, 2228.
- [12] X. Gao, J. Zhang, F. Song, Q. Zhang, Y. Han, Y. Tan, Chem. Commun. 2022, 58, 4687-4699.
- [13] W. Cai, C. Wang, Y. Chu, M. Hu, Q. Wang, J. Xu, F. Deng, Nat. Commun. 2024, 15, 8736.
- [14] S. Xie, Z. Shen, J. Deng, P. Guo, Q. Zhang, H. Zhang, C. Ma, Z. Jiang, J. Cheng, D. Deng, Y. Wang, Nat. Commun. 2018, 9, 1181.
- [15] M. Xiao, A. Baktash, M. Lyu, G. Zhao, Y. Jin, L. Wang, Angew. Chem. Int. Ed. 2024, 63, e202402004.
- [16] M. Liu, Y. Wang, X. Kong, R. T. Rashid, S. Chu, C.-C. Li, Z. Hearne, H. Guo, Z. Mi, C.-J. Li, Chem 2019, 5, 858-867.
- [17] Y. Li, J. Lu, X. Wang, H. Zhang, X. Wu, K. H. L. Zhang, J. Ye, D. Zhan, ChemCatChem 2019, 11, 2277-2282.
- [18] Z. Li, A. Ivanenko, X. Meng, Z. Zhang, J. Hazard. Mater. 2019, 380, 120822.

- [19] S. Luo, H. Song, F. Ichihara, M. Oshikiri, W. Lu, D.-M. Tang, S. Li, Y. Li, Y. Li, P. Davin, T. Kako, H. Lin, J. Ye, J. Am. Chem. Soc. 2023, 145, 20530-20538.
- [20] G. Chen, L. Li, Y. Liu, Z. Li, Y. Hu, H. Wang, X. Zhang, Y. Xie, Angew. Chem. Int. Ed. 2025, e202507093.
- [21] L. Wang, Y. Sun, F. Zhang, J. Hu, W. Hu, S. Xie, Y. Wang, J. Feng, Y. Li, G. Wang, B. Zhang, H. Wang, Q. Zhang, Y. Wang, Adv. Mater. 2023, 35, 2205782.
- [22] X. Zhang, Y. Liu, X. Wang, Y. Zhou, X. Wang, S. Chen, Y. Ren, D. Ding, F. Tian, Y. Li, F. Huang, D. Luo, J. Environ. Chem. Eng. 2024, 12, 114099.
- [23] W. Yan, N. Li, Z. Yan, Z. Wang, Catal. Sci. Technol. 2023, 13, 1482-1487.
- [24] B. Wu, B. Jiang, C. Guo, J. Zhang, Q. Li, N. Wang, Z. Song, C. Tian, M. Antonietti, H. Fu, Angew. Chem. Int. Ed. 2025, 64,
- [25] Y. Pi, W. Lin, J. Li, J. Yang, Z. Zengcai, Q. Chen, J. Guo, T. Wang, Angew. Chem. Int. Ed. 2025, 64, e202423269.
- [26] Y. Qian, Q. Zhan, Z. Li, R. Tan, X. Mu, L. Li, C.-J. Li, J. Am. Chem. Soc. 2025, 147, 10349-10356.
- [27] H. Zhang, S. Xie, J. Hu, X. Wu, Q. Zhang, J. Cheng, Y. Wang, Chem. Commun. 2020, 56, 1776–1779.
- [28] J. Liang, Q. Song, H. Zhang, Z. Liu, Y. Li, Z. Jiang, X. W. D. Lou, C.-S. Lee, Angew. Chem. Int. Ed. 2024, 63, e202318236.
- [29] J. Luo, C. Zhu, J. Li, J. Jin, N. E. Soland, P. W. Smith, Y. Shan, A. M. Oddo, A. L. Maulana, L. Jayasinghe, X. Chen, T. Wang, J.-A. Lin, E. Lu, B. Schaefer, M. Schmalzbauer, R. Zhang, F. Seeler, C. Lizandara-Pueyo, J. Guo, P. Yang, J. Am. Chem. Soc. 2025, 147, 3428-3437.
- [30] X. Wang, J. He, Y.-N. Wang, Z. Zhao, K. Jiang, W. Yang, T. Zhang, S. Jia, K. Zhong, L. Niu, Y. Lan, Chem. Rev. 2024, 124, 10192-10280.
- [31] L. Capaldo, T. Noël, D. Ravelli, Chem Catal 2022, 2, 957–966.
- [32] B. J. Shields, A. G. Doyle, J. Am. Chem. Soc. 2016, 138, 12719-12722.
- [33] Y. Itabashi, H. Asahara, K. Ohkubo, Chem. Commun. 2023, 59, 7506-7517.
- [34] L. Capaldo, D. Ravelli, Eur. J. Org. Chem. 2017, 2017, 2056-
- [35] G. Lei, M. Xu, R. Chang, I. Funes-Ardoiz, J. Ye, J. Am. Chem. Soc. 2021, 143, 11251-11261.
- [36] Q. Yang, Y.-H. Wang, Y. Qiao, M. Gau, P. J. Carroll, P. J. Walsh, E. J. Schelter, Science 2021, 372, 847-852.
- [37] Q. Li, Y. Xia, C. Yang, K. Lv, M. Lei, M. Li, Chem. Eng. J. 2018, 349, 287-296.
- [38] L. Wang, J. Guan, H. Han, M. Yao, J. Kang, M. Peng, D. Wang, J. Xu, J. Hao, Appl. Catal. B Environ. 2022, 306, 121130.
- [39] D. Luo, L. Peng, Y. Wang, X. Lu, C. Yang, X. Xu, Y. Huang, Y. Ni, J. Mater. Chem. A 2021, 9, 908-914.
- [40] Z.-L. Liu, M.-R. Zhang, G.-X. Dong, M. Zhang, T.-B. Lu, Sol. RRL 2023, 7, 2300300.
- [41] Z. Wu, M. Li, D. R. Mullins, S. H. Overbury, ACS Catal. 2012, 2, 2224-2234.
- [42] H. Li, T. Hu, N. Du, R. Zhang, J. Liu, W. Hou, Appl. Catal. B Environ. 2016, 187, 342-349.
- [43] A. R. Martínez, M. C. Rodríguez, I. Rodríguez-García, L. P. Morales, R. N. R. Maecker, Chin. J. Catal. 2017, 38, 1659-
- [44] J. Guo, L. Mao, J. Zhang, C. Feng, Appl. Surf. Sci. 2010, 256, 2132-2137.
- [45] X. Wang, P. Cui, C. Xia, L. Wu, Angew. Chem. Int. Ed. 2021, 60, 12298-12303.
- [46] C.-Y. Huang, J. Li, C.-J. Li, Nat. Commun. 2021, 12, 4010.



Communication



- [47] C. M. So, S. Kume, T. Hayashi, J. Am. Chem. Soc. 2013, 135, 10990–10993.
- [48] M. Simmons, J. F. Hartwig, Angew. Chem. Int. Ed. 2012, 51, 3066–3072.
- [49] M. Gómez-Gallego, M. A. Sierra, Chem. Rev. 2011, 111, 4857– 4963
- [50] J. C. Rienstra-Kiracofe, G. S. Tschumper, H. F. Schaefer, S. Nandi, G. B. Ellison, Chem. Rev. 2002, 102, 231– 282
- [51] G. Hippargi, P. Mangrulkar, A. Chilkalwar, N. Labhsetwar, S. Rayalu, Int. J. Hydrogen Energy 2018, 43, 6815–6823.
- [52] L. Huang, R. Li, R. Chong, G. Liu, J. Han, C. Li, Catal. Sci. Technol. 2014, 4, 2913.

Manuscript received: May 19, 2025 Revised manuscript received: June 10, 2025 Accepted manuscript online: June 11, 2025 Version of record online: ■■, ■■ 15217373, 0, Downloaded from https://onlinelibrary.wielyc.com/doi/10.002/anie.202510993 by Tianjin University Of, Wiley Online Library on [24.062025]. See the Terms and Conditions (https://onlinelibrary.wielyc.com/terms-und-conditions) on Wiley Online Library for rules of use; OA articles are governed by the applicable Creative Commons. Licensea

Communication

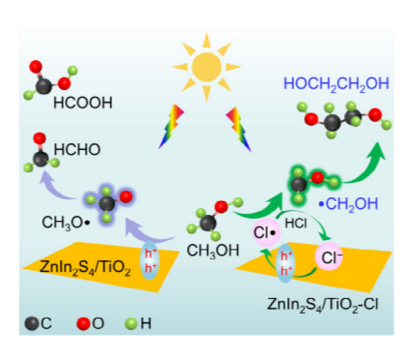
Communication

Photocatalysis

G.-X. Dong, M.-R. Zhang, S.-X. Yuan, M. Zhang*, T.-B. Lu* _____ e202510993

Chlorine Radical-Mediated Photocatalytic C—C Coupling of Methanol to Ethylene Glycol with Near-Unity Selectivity

A Z-scheme ZnIn₂S₄/TiO₂-Cl photocatalyst pioneers selective methanol C—H bond activation under mild conditions, achieving 96.7% ethylene glycol selectivity. By leveraging photogenerated holes to cycle Cl⁻/Cl•, the system drives hydrogen abstraction for C—H cleavage and suppresses overoxidation, steering methanol valorization from traditional C₁ pathways to sustainable C₂ chemistry.



15217373, 0, Downloaded from https://onlinelibrary.wielyc.com/doi/10.002/anie.202510993 by Tianjin University Of, Wiley Online Library on [24.062025]. See the Terms and Conditions (https://onlinelibrary.wielyc.com/terms-und-conditions) on Wiley Online Library for rules of use; OA articles are governed by the applicable Creative Commons. Licensea